RCSI Leading the world to better health

Royal College of Surgeons in Ireland

repository@rcsi.com

Rapid healing of a critical-sized bone defect using a collagen-hydroxyapatite scaffold to facilitate low dose, combinatorial growth factor delivery.

AUTHOR(S)

David Walsh, Rosanne Raftery, Gang Chen, Andreas Heise, Fergal O'Brien, Sally-Ann Cryan

CITATION

Walsh, David; Raftery, Rosanne; Chen, Gang; Heise, Andreas; O'Brien, Fergal; Cryan, Sally-Ann (2020): Rapid healing of a critical-sized bone defect using a collagen-hydroxyapatite scaffold to facilitate low dose, combinatorial growth factor delivery.. figshare. Journal contribution. https://doi.org/10.25419/rcsi.11673720.v1

DOI

10.25419/rcsi.11673720.v1

LICENCE

CC BY-NC-SA 4.0

This work is made available under the above open licence by RCSI and has been printed from https://repository.rcsi.com. For more information please contact repository@rcsi.com

URL

https://repository.rcsi.com/articles/Rapid_healing_of_a_critical-sized_bone_defect_using_a_collagen-hydroxyapatite_scaffold_to_facilitate_low_dose_combinatorial_growth_factor_delivery_/11673720/1

Rapid healing of a critical-sized bone defect using a collagen-hydroxyapatite scaffold to facilitate low dose, combinatorial growth factor delivery

Running Title: Rapid bone tissue regeneration using a dual protein loaded collagen scaffold

David P. Walsh[*1-4], *Rosanne M. Raftery*[*1-4], *Gang Chen*[5], Andreas Heise[6,7], *Fergal J. O'Brien*[# 1-4,7], *Sally-Ann Cryan*[# 1-4,7].

[1]*Drug Delivery & Advanced Materials Team*, School *of Pharmacy, RCSI, Dublin, Ireland*

[2]*Tissue Engineering Research Group, Department of Anatomy, RCSI, Dublin, Ireland*

[3]*Trinity Centre for Bioengineering, Trinity College Dublin (TCD), Dublin, Ireland*

[4]*Advanced Materials and Bioengineering Research (AMBER) Centre, RCSI & TCD*

[5]*Department of Physiology and Medical Physics, Centre for the Study of Neurological Disorders, Microsurgical Research and Training Facility (MRTF), RCSI, Dublin, Ireland*

[6]*Department of Chemistry, RCSI, Dublin, Ireland*

[7]*Centre for Research in Medical Devices (CURAM), RCSI, Dublin and National University of Ireland, Galway, Ireland*

**D.P Walsh & R.M Raftery contributed equally to this work.*

#F.J O'Brien & SA-Cryan are joint senior authors of this work.

Corresponding Author:

Professor Sally-Ann Cryan

School of Pharmacy,

Royal College of Surgeons in Ireland,

1st Floor, Ardilaun House (Block B), Dublin 2, Ireland

Tel: 00353-(0)1-4022741

Email: scryan@rcsi.ie

Abstract

The healing of large, critically sized, bone defects remains an unmet clinical need in modern orthopaedic medicine. The tissue engineering field is increasingly using biomaterial scaffolds as 3D templates to guide the regenerative process which can be further augmented via the incorporation of recombinant growth factors. Typically, this necessitates supraphysiological doses of growth factor to facilitate an adequate therapeutic response. Herein, we describe a cell-free, biomaterial implant which is functionalised with a low dose, combinatorial growth factor therapy that is capable of rapidly regenerating vascularised bone tissue within a critical sized rodent calvarial defect. Specifically, we demonstrate that the dual delivery of the growth factors bone morphogenetic protein-2 (osteogenic) and vascular endothelial growth factor (angiogenic) at a low dose (5 µg /scaffold) on an osteoconductive collagen-hydroxyapatite scaffold is highly effective in healing these critical-sized bone defects. The high affinity between the hydroxyapatite component of this biomimetic scaffold and the growth factors functions to sequester them locally at the defect site. Using this growth factor-loaded scaffold, we show complete bridging of a critical sized calvarial defect in all specimens at a very early time-point of 4 weeks, with a 28-fold increase in new bone volume and 7-fold increase in new bone area compared to a growth factor-free scaffold. Overall, this study demonstrates that a collagen-hydroxyapatite scaffold can be used to locally harness the synergistic relationship between osteogenic and angiogenic growth factors to rapidly regenerate bone tissue without the need for more complex controlled delivery vehicles or high total growth factor doses.

Keywords: Tissue engineering, bone tissue, collagen scaffold, bone morphogenetic protein 2, vascular endothelial growth factor,

Introduction

Bone tissue possesses a unique ability for self-repair in response to minor injuries or trauma (Fröhlich et al., 2008). However, the healing of large bone defects which are above a critical size remains an unmet clinical need in modern orthopaedics (Verrier et al., 2016). Bone tissue engineering (BTE) aims to facilitate and accelerate the body's natural healing capacity via the use of biomaterial scaffolds which encourage autologous host cells to proliferate, differentiate and instigate the repair process. Previously, we have described the development and application of a highly porous, collagen-hydroxyapatite (CHA) composite scaffold for bone tissue repair (Gleeson, Plunkett, & O'Brien, 2010). The incorporation of the ceramic hydroxyapatite (HA) component into a collagen scaffold functioned to create a construct which is osteoconductive, possesses optimal mechanical properties for bone tissue formation and is both biocompatible and biodegradable. Indeed our laboratory has demonstrated the significant regenerative capacity of this CHA scaffold in the healing of bone defects using several *in vivo* models including rodents (Gleeson et al., 2010), rabbits (Lyons, Gleeson, Partap, Coghlan, & O'Brien, 2014) and more recently, in a thoroughbred filly (David et al., 2015).

While this biomimetic CHA scaffold has, to date, demonstrated significant potential in the healing of small bone defects, it is recognised that for the healing of larger defects, an additional therapeutic stimulus may be required to both rapidly enhance the deposition of new bone and also ensure the formation of an adequate vascular network (Raftery et al., 2017). Therefore, the application of a growth factor (GF) in combination with biomaterials to augment their regenerative capacity is increasingly becoming a focus of next generation BTE strategies. Perhaps the best-known example is INFUSE® bone graft (Medtronic) which is used to promote lumbar spinal fusion in humans and consists of recombinant human BMP-2 (rhBMP-2) soak-loaded onto a collagen sponge. While approved clinically, INFUSE® exhibits poor GF release kinetics and therefore requires supraphysiological dosing of BMP-2 (up to 12 mg rhBMP-2 per 7.62cm x 10.16cm collagen sponge) which has been linked to ectopic bone formation, cytotoxicity, renal complications and a potential increased malignancy risk (Carragee, Hurwitz, & Weiner, 2011; Zara et al., 2011). These limitations have prompted extensive research studies into more advanced platforms for tissue repair which attempt to confer enhanced spatiotemporal control of GF release locally. Techniques used to achieve these properties include GF encapsulation within microparticles (E. Quinlan, A. Lopez-Noriega, et al., 2015) or delivery via nanoparticles (Wei, Jin, Giannobile, & Ma, 2007; Yilgor, Tuzlakoglu, Reis, Hasirci, & Hasirci,

2009) as well as the alternative approach of delivering gene therapeutics which encode for a specific GF (R. M. Raftery et al., 2016; D. P. Walsh, Heise, O'Brien, & Cryan, 2017; David P. Walsh et al., 2018).

The individual delivery of rhBMP-2 (Endo et al., 2006; Ono et al., 2004; Park et al., 2007) or recombinant human vascularised endothelial growth factor (rhVEGF) (Keeney, van den Beucken, van der Kraan, Jansen, & Pandit, 2010; E. Quinlan, A. Lopez-Noriega, et al., 2015) on biomaterial scaffolds has previously been extensively trialled for the healing of large bone defects, with promising results to date. Increasingly however, the use of combinatorial GF therapy, which involves the dual application of osteogenic and angiogenic GFs is being used as a potentially more efficient therapy for the recapitulation of mature vascularized bone via harnessing of the osteogenic-angiogenic coupling effect (Peng et al., 2002). However, large doses of GF have been required to stimulate adequate bone tissue regeneration using this approach. For example, *Patel et al.* used a porous poly(propylene fumarate) scaffold of 8mm diameter and 1mm height to deliver 14 µg of a dual GF mixture (2 µg rhBMP-2 & 12 µg rhVEGF) to achieve bone regeneration in a critically sized, rodent calvarial defect (Patel et al., 2008).

In acknowledgement of the previous work in this research field which has established the benefits of combinatorial GF delivery, the overall objective of this study was to develop a cell-free, biomimetic, low dose, dual-GF loaded scaffold via the soak-loading of an osteoconductive CHA scaffold with an osteoinductive dual-GF cargo of rhBMP-2 and rhVEGF. The use of combinatorial GF therapy and its previously demonstrated effectiveness in the regeneration of vascularised bone tissue underpinned our low dose approach (Patel et al., 2008; Patterson et al., 2010). Furthermore, it is established within the literature that ceramic materials such as hydroxyapatite (HA) possess a naturally high binding affinity for GFs (Lo, Ulery, Ashe, & Laurencin, 2012; Wang, Zhou, Hong, & Zhang, 2012). As such, we hypothesised that the CHA scaffold would function as a carrier for the dual-GF cargo, thereby sequestering the GFs locally at the defect site and facilitating the use of a relatively low, 5 µg GF dose per scaffold which consisted of 2.5 µg of rhBMP-2 and 2.5 µg of rhVEGF.

Materials & Methods

All materials were supplied by Sigma-Aldrich, Ireland unless otherwise stated.

Scaffold fabrication

Collagen and CHA scaffolds were fabricated as previously described (Gleeson et al., 2010; Rosanne M. Raftery et al., 2016). Collagen scaffold slurry; A collagen slurry was formed via the addition of 1.8g of collagen (Southern Lights Biomaterials (SLB), New Zealand) to 360ml of 0.05M glacial acetic acid (HOAc). This mixture was blended at 15,000rpm for 90 minutes using an overhead blender (Ultra Turrax T18 overhead blender, IKA Works Inc., USA) maintained at 4^0C via a cooling system (Lauda WKL250). CHA scaffold slurry; As per the patented protocol, 1.8g of collagen (SLB, New Zealand) was added to 320ml of 0.5M HOAc with blending for 90 minutes as described above. 3.6g (200 wt.%) of hydroxyapatite was dissolved in 40ml of 0.5M HOAc and added slowly to the collagen slurry at a rate of 10ml/hour while maintaining a dispersion at 15,000rpm. Following the addition of all the hydroxyapatite the slurry was blended further for 60 minutes. Following slurry formation for each scaffold type, gas was removed using a vacuum pump and the slurries were freeze dried (Advantage EL, Vis-Tir Co. Gardiner NY) to a final temperature of -10^0C using a previously optimised freeze drying profile (O'Brien, Harley, Yannas, & Gibson, 2004). Following fabrication, scaffolds were cross-linked dehydrothermally (DHT) at 105°C for 24 hours in a vacuum oven (Vacucell 22; MMM, Germany) and subsequently cut into dry, cylindrical sections of 8mm diameter and 1.5mm height. These dimensions were designed to be press-fit into the calvarial defect but also to mimic the thickness of natural rodent cortical bone.

Dual growth factor-loaded scaffold preparation

Prior to use, each scaffold was rehydrated in 2mL of PBS and then chemically cross-linked using *a* mixture of 14mM N-(3-Dimethylaminopropyl)-N'-ethylcarbodiimide hydrochloride (EDC) and 5.5 mM N-hydroxysuccinimide (NHS). Each scaffold was then placed in 2mL of fresh PBS and placed on a plate rocker for approximately 30 minutes to remove any excess EDC and NHS as per established protocols in our laboratory (Haugh, Murphy, McKiernan, Altenbuchner, & O'Brien, 2011). This wash step was repeated a total of five times for each scaffold to ensure all crosslinkers had been removed from the scaffold. rhBMP-2 and rhVEGF-165 proteins were obtained from R&D systems (Abingdon, UK). Both proteins were reconstituted in sterile, 4mM HCL at the concentrations of 100 µg/mL (rhBMP-2) and 500 µg/mL (rhVEGF). To form a dual

GF-loaded scaffold, the scaffolds were first removed from PBS and excess liquid removed using a pipette. 25 µL of rhBMP-2 solution (contains 2.5 µg rhBMP-2 protein) was mixed with 5 µL of rhVEGF solution (contains 2.5 µg rhVEGF protein). 15 µL of this GF mixture was soak-loaded onto one side of the CHA scaffold. The scaffold was incubated at 37˚C for 15 minutes, carefully inverted and the remaining 15 µL of GF mixture added to the second side. Following a subsequent 15-minute incubation at 37˚C the scaffolds were ready for use. The total dose of GF delivered per scaffold was 5 µg which included equal doses of rhBMP-2 (2.5 µg) and rhVEGF (2.5 µg).

Growth factor release kinetics and functionality

Dual GF-loaded collagen and CHA scaffolds were formed as above. To compare the GF release profile from each scaffold and determine the effect that the incorporation of HA has, each scaffold type (n=3) was placed in 2mL of PBS and incubated at 37°C. At pre-determined time-points of 1, 2, 3, 4, 5, 10, 15, 20, 25 and 30 days, 1mL of PBS was removed and GF content was quantified using enzyme-linked immunosorbent assay (ELISA) for human BMP-2 and human VEGF (Biotechne, UK) as per the protocol. To examine the ability of the GF-loaded scaffolds to promote osteogenesis, rodent MSCs (Cyagen) were seeded onto GF-loaded collagen and CHA scaffolds as well as GF-free collagen and CHA controls. Here, approximately $2x10^5$ MSCs (passage 5) were seeded onto each side of the scaffold surface as previously described (D. P. Walsh et al., 2017). Dulbecco's modified eagles medium supplemented with 10% FBS, 1% penicillin/streptomycin, 10 mM β-glycerophosphate, 50 µM ascorbic acid 2-phosphate and 100 nM dexamethasone was added to the cells and changed every three days until day 30. Calcium content was quantified at day 30 using a Stanbio calcium assay (Calcium CPC Liquicolour, Stanbio Inc., USA). Briefly, media was removed and the cells were rinsed with 1mL of PBS. One mL of 0.5 M HCl was then added to each well and the contents of each well were scraped into microcentrifuge tubes and left to shake overnight at 4 °C. Calcium levels were then quantified according to the manufacturer's instructions against a standard curve.

Surgical procedure

A critical sized rodent calvarial defect model was used in this study. This model is utilised in almost half of all critical defect studies for bone regeneration (O'Loughlin et al., 2008) and is well established within our laboratory (Alhag et al., 2012; Lyons et al., 2010). There were two study groups used; 1) a GF-free scaffold group (n=8) and 2) a dual GF-loaded scaffold group (n=8), total animals =16. Ethical approval for this study was given by the Research Ethics Committee of the Royal College of Surgeons in Ireland (REC #1205) and a project license was granted by

the Health Products Regulatory Authority (HPRA) (License # AE19127/P036) in compliance with EU directive 2010/EU/63. Anaesthesia was induced with intraperitoneal medetomidine hydrochloride (0.3 mg/kg) and ketamine hydrochloride (70 mg/kg) and maintained with inhalational isoflurane (0.5–2%) and oxygen. The skin of the head was shaved and cleaned using 70% ethanol and chlorohexidine. Analgesia (Buprenorphine – 0.05 mg/kg) and 2mLs of saline were administered subcutaneously before the animal was placed in the prone position on a heated aseptic operating platform prior to draping. A 2.5mm sagittal skin incision over the calvarium was made and the soft tissues and periosteum were dissected using a blunt technique and the calvarium was exposed using retractors. A 7mm trephine drill was used to create a circular transosseous defect under constant irrigation with 0.9% NaCl as previously described by us (Raftery et al., 2017).

Each scaffold (GF-free or dual GF-loaded) was implanted into the defect and the periosteum was sutured using Vicryl® 4-0 absorbable sutures (Ethicon, USA). The wound was further secured using a topical skin adhesive (n-butyl cyanoacrylate) (Vetbond™). Post-operatively, atipamezole hydrochloride (0.05 mg/kg) was administered subcutaneously to reverse sedation. Antibiotic prophylaxis was administered in the drinking water in the form of Baytril® (enrofloxacin) (5 mg/kg) for 3 days post-surgery. At four weeks post implantation the animals were euthanized by CO_2 asphyxiation followed by cervical dislocation. A 20mm x 20mm segment of calvarium containing the defect site was resected using a dental saw (Osung Dental, USA). The explants were washed in PBS until clear washout was observable before fixation in 10% formalin. Scaffolds were then stored in PBS at 4˚C prior to analysis.

Microcomputed tomography (MicroCT) analysis

MicroCT analysis was used to both qualitatively and quantitatively assess new bone formation within each defect for all animals (n=16 total). Scans of the 20mm x 20mm excised calvarial were performed on a Scanco Medical 40 MicroCT system (Scanco Medical, Switzerland) with a voxel resolution of 12 µm, a 70kVP x-ray source and 112 µA current. A reconstructed 3D tomogram was formed using Scanco software package which consisted of 300 sliced, 2D projection images (a threshold of 140, scale from 0 to 1000, density of 257.99 mg HA/cm). To ensure only new bone was being assessed, a 6mm region of interest (ROI) within each defect was chosen for analysis. Bone formation was expressed as a percentage of bone volume over total volume (%BV/TV), trabecular number (Tb.N), trabecular thickness (Tb.Th) and trabecular spacing (Tb.Sp) within this ROI.

Histological assessment

To corroborate the microCT analysis, both qualitative and quantitative histology was performed on each explant. Each specimen was submerged in Decalcifying Solution-Lite® for approximately 13 hours to remove all calcium. Specimens were processed overnight using an automatic tissue processor (ASP300, Leica, Germany). The defect was then bisected, and each specimen embedded in a paraffin block. Each block was cut using a rotary microtome (Microsystems GmbH, Germany) into 7 µm sections from the mid-section of each block. Sections were mounted onto poly(L-lysine) slides and dried overnight in an oven at 60°C. Histological assessment was performed using Haematoxylin & Eosin (H&E) staining and Masson's (MT) Trichrome staining. Images of each section were acquired and digitized using a transmitted light microscope (Nikon Microscope Eclipse 90i with NIS elements software v3.06) (Nikon instruments, Holland). Quantitative histomorphometrical analysis was carried out on n=6 sections from each specimen using the H&E stain (total specimens = 16, quantified sections = 96) to quantify the healing response as previously described (Raftery et al., 2017).

Immunofluorescence staining for neovascularisation

To determine if the inclusion of VEGF protein in the dual GF-loaded scaffold resulted in enhanced neovascularisation within the defect we assessed the presence of platelet endothelial cell adhesion marker (PECAM/CD31) within each group. Cross-sections of decalcified, paraffin-embedded tissue from each defect were deparaffinised and hydrated to 0.05% Tween 20 in PBS. Antigen retrieval was carried out using a citrate-based buffer (Vector labs) and endogenous peroxidase activity was quenched using hydrogen peroxidase (Abcam) before incubation in blocking buffer for 1 h. The specimens were washed in 0.05% Tween 20 in PBS and incubated in rabbit anti-rat polyclonal antibody to CD31 (Abcam) at a dilution of 1:1000 in 1% BSA in PBS overnight at 4°C. A goat anti-rabbit IgG secondary antibody tagged with Alexa Fluor 647 (Abcam) was used at a concentration of 1:500 and incubated for 1 h at room temperature. The sections were counterstained using Hoescht 33258 (Sigma) and mounted using Fluoromount (Sigma). The number of vessels found in 3 random images within the defect site (n=3 sections per animal; n=4 animals per treatment group) were imaged using a Nikon Microscope Eclipse 90i with NIS Elements software v3.06, Nikon instruments Europe, The Netherlands) and quantified (blinded) using ImageJ software.

Statistical analysis

All results are expressed as the mean ± standard deviation (SD). Each experiment was performed independently in triplicate unless otherwise stated. Each *in vivo* experimental group consisted of n=8 animals (n=16 animals total). Statistical significance was determined using

either an unpaired T-test when two groups were being compared or a one-way ANOVA plus Tukey *post-hoc* test when three or more groups were being compared. Values of $p \leq 0.05$ were considered statistically significant where *$p<0.05$, **p0.01, ***$p<0.001$ & ****$p \leq 0.0001$. Data was analysed using GraphPad Prism v6.1 software.

Results

The incorporation of a ceramic hydroxyapatite component in a collagen scaffold facilitates the sustained release of growth factors over a 30-day period

The release profile of BMP-2 (*Figure 1A*) and VEGF (*Figure 1B*) proteins from the dual GF-loaded collagen and CHA scaffolds demonstrated that the CHA scaffold facilitated sustained release of therapeutic proteins over a prolonged 30-day period. Using this CHA scaffold, a low burst release of just 30% of the loaded BMP-2 and VEGF protein doses was evident within the first five days. In contrast, release of both BMP-2 and VEGF proteins from the collagen scaffold was rapid, with a burst release of 70-80% of the loaded protein dose within the first five days. At day 30, only 60% of the loaded BMP-2 dose and 50% of the loaded VEGF dose had been released from the CHA scaffold while approximately 88% of the loaded BMP-2 and 70% of the loaded VEGF dose had been released from the collagen scaffold.

Sustained release of therapeutic proteins from a dual growth factor loaded CHA scaffold facilitates enhanced MSC mediated osteogenesis

To assess if the sustained release profile observed from a CHA scaffold for both BMP-2 and VEGF translated into enhanced MSC mediated osteogenesis we quantified the level of calcium deposition per scaffold at 30 days post seeding with MSCs. For both GF-loaded scaffolds, the addition of BMP-2 & VEGF enhanced MSC mediated osteogenesis *in vitro* over their corresponding GF-free scaffolds *(Figure 2).* The GF-loaded CHA scaffold resulted in a significantly higher amount of calcium per scaffold compared to the GF-loaded collagen scaffold ($p<0.001$). In fact, this GF-loaded CHA scaffold resulted in the highest level of MSC mediated mineral deposition of all scaffolds assessed, with over 2000 µg calcium per scaffold produced at day 30 which was significantly increased over all other scaffold groups ($p<0.001$).

Dual growth factor loaded CHA scaffolds facilitate rapid bridging of critical sized bone defects *in vivo* after just four weeks

We next assessed the potential of this dual GF-loaded CHA scaffold to facilitate healing of a critical sized, rodent calvarial bone defect *in vivo* with comparative analysis against a GF-free CHA scaffold. Due to their reduced capacity to stimulate MSC mediated osteogenesis, neither the GF-free collagen or the dual GF-loaded collagen scaffolds

were brought forward to this study. At the early time-point of four weeks, 3D reconstructions generated using microCT qualitatively demonstrated enhanced bone tissue regeneration in each specimen for the dual GF-loaded CHA scaffold group (n = 8) *(Figure 3B)* compared to that of the GF-free CHA scaffold group (n=8) *(Figure 3A).* In all GF-loaded specimens, complete bridging of the defect with *de novo* synthesized bone was clearly evident. In contrast, little to no healing was yet evident in the GF-free specimens. Quantitative assessment of a 6mm region of interest (ROI) was selected to determine the healing response. *Figure 3C* displays the new bone volume (BV) calculated as a percentage of total volume (TV) of the ROI (%BV/TV or bone volume fraction). The quantitative results corroborate this data in that a significantly increased bone volume fraction was evident in animals treated with the GF-loaded scaffold (59.3 ± 15.1% BV/TV) compared to that of the GF-free scaffold (2.1 ± 0.9% BV/TV) ($p<0.0001$). This increase in bone volume fraction equates to a 28-fold increase in new bone formation by the GF-loaded CHA scaffold compared to a GF-free CHA scaffold. Analysis of trabeculae characteristics in terms of trabecular number *(Figure 3D)*, trabecular thickness *(Figure 3E)* and trabecular spacing *(Figure 3F)* within this ROI indicated that the bone tissue formed using the GF-loaded scaffold contained a significantly increased number of trabeculae ($p<0.0001$) which were both significantly thicker ($p<0.001$) and closer together ($p<0.01$) compared to the GF-free scaffold group

Histological assessment of each defect revealed the presence of mature, vascularized bone within the dual growth factor-loaded CHA scaffold groups after just four weeks

H&E and MT stains were used to histologically assess new bone formation. H&E stains cell nuclei purple, extracellular matrix pink and bone dark pink/red while MT stains collagen/mineralised bone blue and osteoid red. H&E stained sections of the GF-free CHA scaffold specimens *(Figure 4A (i))* illustrated a highly cellularised scaffold present in most specimens but a lack of new bone tissue at this early timepoint. Similarly, minimal deposition of mineralised bone was evident after MT staining within the defect in this group *(Figure 4A (iii))*. The scaffold itself did not appear well integrated into the defect in multiple specimens, with a discernible boundary between the scaffold and host tissue evident. High magnification images corroborated these observations (*Figure 4A (ii & iv)*) as the specimens displayed a high level of cellular infiltration, but minimal osteoid deposition or new bone matrix.

In contrast, the GF-loaded CHA scaffold group demonstrated extensive evidence of new bone formation using both H&E (*Figure 4B (i))* and MT (*Figure 4B (iii))* staining. New bone tissue was evident throughout the defect, with extensive evidence of osteoid and mineralised bone tissue present. The GF-loaded CHA scaffold specimens contained considerable calcified bone matrix, histologically representing mature lamellar bone tissue. High magnification images *(Figure 4B (ii & iv)* further corroborated these results, demonstrating the presence of mature, mineralised bone tissue.

Histomorphometry was used to quantify the area of new bone within each defect of the H&E stained sections *(Figure 4C)*. These quantitative results corroborate the microCT analysis in that the GF-loaded CHA scaffolds resulted in a highly significant, 7-fold increase in new bone area ($2.71 \times 10^6 \pm 4.5 \times 10^5$ μm^2) compared to that of the GF-free scaffold group ($3.7 \times 10^5 \pm 7.5 \times 10^4$ μm^2) at this early timepoint of four weeks ($p<0.0001$).

Finally, immunofluorescence staining was used to assess the degree of neovascularisation within each scaffold via the detection of CD31 positive endothelial cells *(Figure 4D)*. Reduced positive staining for CD31 (red fluorescence) was evident in the GF-free CHA scaffold group *(Figure 4D (i))* in contrast with the GF-loaded CHA scaffold group *(Figure 4D (ii))* which demonstrated intense positive staining. When quantified, the GF-loaded CHA scaffold demonstrated a 15-fold increase in the average blood vessel density per image assessed compared to the GF-free scaffold ($p<0.01$) *(Figure 4E)*.

Discussion

There remains an unmet clinical need for the treatment of large, critical sized bone tissue defects. Increasingly, BTE strategies are focused on the incorporation of GFs into biomaterial implants with the aim of stimulating and augmenting the body's natural regenerative capacity (Lee, Silva, & Mooney, 2011). Previously, the individual delivery of BMP-2 (Geiger, Li, & Friess, 2003) or VEGF (E. Quinlan, A. Lopez-Noriega, et al., 2015) GFs on a collagen scaffold has demonstrated significant bone tissue regenerative potential. In these instances, complex delivery technologies such as the use of nanoparticles (Wei et al., 2007) have been combined with tissue engineering scaffolds to achieve optimal spatiotemporal control of GF release and thereby enhance tissue repair. More recently however, combinatorial GF therapy, whereby two synergistic GFs are employed to further enhance tissue regeneration has emerged as a compelling BTE strategy to recapitulate vascularised bone (Curtin et al., 2015; Koh et al., 2008). Building on these previous experiments, the present study aimed to develop a low dose, dual GF-loaded CHA scaffold which would be capable of rapidly regenerating bone tissue *in vivo* at the early timepoint of 4 weeks. To achieve this aim, we sought to harness the well documented therapeutic synergism of the dual delivery of BMP-2 and VEGF GFs, commonly referred to as osteogenic-angiogenic coupling (Peng et al., 2002; Raftery et al., 2017).

A cell-free (prior to implantation), biomimetic and osteoconductive CHA scaffold was chosen as the optimal matrix to promote bone tissue regeneration due to its well documented efficacy in the healing of bone defects *in vivo (David et al., 2015; Gleeson et al., 2010; Lyons et al., 2014).* The use of this scaffold offered an alternative approach to two commonly employed methodologies in BTE – namely the use of controlled delivery technologies and the use of supraphysiological protein doses. We have previously demonstrated that the regenerative capacity of this CHA scaffold can be further enhanced via the incorporation of individual therapeutic growth factors such as rhBMP-2 either encapsulated within PLGA/alginate microparticles (Elaine Quinlan et al., 2015) or added during the fabrication process (Quinlan, Thompson, Matsiko, O'Brien, & Lopez-Noriega, 2015), or rhVEGF, encapsulated within spray-dried alginate microparticles (E. Quinlan, A. Lopez-Noriega, et al., 2015). Indeed, growth factors such as rhBMP-2 are commonly applied to biomaterial scaffolds for bone tissue regeneration, with doses ranging from 1 µg rhBMP-2 per scaffold (Ben-David et al., 2013; Jeon, Song, Kang, Putnam, & Kim, 2007) up to 30 µg (Martínez-Sanz et al., 2011) depending on the scaffold (porous solid material or hydrogel) used. INFUSE®, one of the leading TE based strategies for bone tissue regeneration, is loaded with doses ranging from 4.2 mg rhBMP-2 up to 12 mg rhBMP-2 depending on the size of the graft required (McKay, Peckham, & Badura, 2007).

These high doses which are used in INFUSE® have been linked to ectopic bone formation, renal complications, cytotoxicity and a potential increased malignancy risk (Carragee et al., 2011; Zara et al., 2011).

Within the literature, there are numerous reports of the ability of calcium phosphates to naturally absorb and enrich native BMP-2 (Yuan et al., 1998) as well as VEGF (Kim et al., 2013) *in vivo.* As such, we hypothesised that the HA component of the CHA scaffold could be used to sequester the dual-GF cargo locally. This would function to locally harness the osteogenic-angiogenic coupling effect, thereby enhancing bone tissue repair without the requirement for controlled release technologies such as microparticles whilst permitting the use of a relatively low protein dose (5 µg/scaffold) to facilitate the tissue regeneration process. Furthermore, this should function to mitigate many of the side effects commonly observed with products such as INFUSE® bone graft.

In agreement with this, we demonstrate that sustained release of bioactive rhBMP-2 and rhVEGF growth factors can be achieved over a prolonged 30-day period *in vitro* when they were co-loaded onto the CHA scaffold. In contrast, collagen only scaffolds lacking this ceramic HA component demonstrated poor release kinetics, with a high burst release of 70-80% of the loaded protein dose within the first five days. This uncontrolled release profile would make this dual GF-loaded collagen scaffold unsuitable for *in vivo* use due to the risk of "dose dumping" upon implantation (Epstein, 2011, 2013). The prolonged release profile of both rhBMP-2 and rhVEGF from the CHA scaffold is likely mediated by both non-specific electrostatic interactions between cationic charges on the GFs and anionic sites on HA as well as the formation of water bridged hydrogen bonds between the -OH, $-NH_2$ and -COOH groups of the GFs and the HA (Dong, Wang, Wu, & Pan, 2007; Gorbunoff & Timasheff, 1984). Importantly, the GF release kinetics from the CHA scaffold are similar to those obtained using a CHA scaffold containing both rhBMP-2 (Elaine Quinlan et al., 2015) and rhVEGF (E. Quinlan, A. Lopez-Noriega, et al., 2015) within alginate microparticles and the lower dose used in this study was still capable of facilitating significant MSC mediated osteogenesis. Thus, the bioactive, dual GF-loaded CHA scaffold which has been developed in this study, whereby low dose GFs are incorporated via an uncomplicated soak loading procedure minimises the design complexity of the construct. As a result, this reduces both the manufacturing and regulatory burdens associated with its development and enhances the potential for clinical translation.

To assess if these positive *in vitro* attributes of sustained release and enhanced osteogenic activity using the dual GF-loaded CHA scaffold translated *in vivo*, we determined the

regenerative potential of the construct using a critically sized, rodent calvarial defect. Impressively, we demonstrate rapid bridging of the bone defect at the very early timepoint of just 4-weeks post implantation, with a 28-fold increase in new bone volume and a 7-fold increase in new bone area compared to a GF-free CHA scaffold. Furthermore, full defect bridging was observed for each animal treated with the dual GF-loaded CHA scaffold, a critical goal in the healing of all critical fractures. Histomorphometrical analysis of the dual GF-loaded CHA scaffold demonstrated evidence of scaffold resorption with the clear presence of vasculature. Importantly, characteristics indicative of rhBMP-2 over dosing such as excess bone resorption or bone abnormalities (Zara et al., 2011) were not present, further indicating the scaffold was functioning to control the release of the therapeutic GFs *in vivo*. Additionally, the clear increase in vasculature observed for the dual GF-loaded CHA scaffold compared to the GF-free CHA scaffold demonstrated that the rhVEGF cargo was exerting a therapeutic angiogenic effect.

The dual application of rhBMP-2 and rhVEGF has previously been assessed for bone repair *in vivo* using a rodent critical calvarial defect at various dose combinations and using different scaffold types. *Patterson et al.* used a hyaluronic acid hydrogel scaffold (35 µl volume) for the dual delivery of 5 µg rhBMP-2 and 25 µg rhVEGF (Patterson et al., 2010). These authors highlighted enhanced bone mineral volume within the defect using this dual delivery group compared to single delivery of either 5 µg rhBMP-2 or 25 µg rhVEGF within scaffolds at 6 weeks post implantation. *Patel et al.,* used an 8mm x 1mm porous poly(propylene fumarate) scaffold to deliver a dual combination of 2 µg rhBMP-2 and 12 µg pVEGF. Here, the authors controlled the release kinetics of both GFs by loading them within gelatin microparticles before incorporation into the scaffold. At 12 weeks post implantation, this dual release group facilitated an increased number of animals displaying bony bridging and union of the defect compared to single delivery of 2 µg rhBMP-2 or 12 µg rhVEGF (Patel et al., 2008). More recently, more complex controlled release systems specifically designed for tailored GF delivery kinetics have been described by *Subbiah et al.* Here, the authors used a dual delivery system consisting of alginate microcapsules to deliver 3 µg rhBMP-2 and 3 µg rhVEGF. In this study, the rhBMP-2 cargo was encapsulated within poly(lactic-co-glycolic acid) nanoparticles which were subsequently incorporated into the alginate microcapsule, while the rhVEGF was entrapped within the alginate matrix itself. These microcapsules were subsequently loaded into an 8mm x 2mm collagen scaffold. This dual delivery group demonstrated enhanced bone tissue regeneration within the defect at 8 weeks post implantation compared to single delivery of either 3 µg rhBMP-2 on a collagen scaffold or microcapsules loaded with just 3 µg rhBMP-2 on a collagen scaffold.

Impressively, this dual release system facilitated a new bone volume of up to 82% at this 8-week timepoint (Subbiah et al., 2015).

While various levels of bone tissue regeneration have been achieved in the above described literature, the present study indicates that the synergistic osteogenic-angiogenic coupling effect of dual BMP-2-VEGF delivery permits the delivery of a relatively lower total dose of GF on a collagen composite scaffold without compromising the regenerative potential of the construct. Indeed, the formation of new bone tissue represents a highly orchestrated series of events which requires the co-operation of a cascade of growth factors being expressed in a spatiotemporally controlled fashion (Chen, Zhang, & Wu, 2010). Therefore, for the successful recapitulation of bone, the presentation of multiple growth factors at the defect site is likely to result in enhanced functional tissue regeneration (Ingber et al., 2006). Furthermore, this study also offers further insights into our previous work in this area. Previously, we have assessed the regenerative capacity of these CHA scaffolds loaded with individual rhBMP-2 either directly incorporated during fabrication (E. Quinlan, E. M. Thompson, et al., 2015) or encapsulated within alginate or PLGA microspheres (Elaine Quinlan et al., 2015) or with rhVEGF incorporated within alginate microspheres (E. Quinlan, A. Lopez-Noriega, et al., 2015). Interestingly, of all these approaches, the highest level of bone regeneration observed in a critical rodent defect was achieved via the direct incorporation of rhBMP-2 into the scaffold during fabrication, with an approximate new bone volume of ~40% at 8-weeks. This observation suggests that perhaps the use of controlled release methodologies, such as the incorporation of GFs within microcapsules may function to slow the rate at which these GFs are available to stimulate bone tissue regeneration in autologous host cells, with the overall effect being a reduced rate of new bone formation.

Overall, *in vitro*, we confirmed the naturally high affinity between the GFs and the HA material within the scaffold which functioned to facilitate sustained release of the GFs over a 30-day period in comparison to a collagen alone scaffold. Furthermore, this dual GF-loaded CHA scaffold facilitated significantly enhanced MSC mediated osteogenesis compared to a dual GF-loaded collagen scaffold, or respective GF-free scaffolds. *In vivo,* using a critical sized rodent calvarial defect model we demonstrate the significant bone healing capacity of this dual GF-loaded CHA scaffold, with full defect bridging occurring in all specimens assessed and the presence of vasculature at the very early time point of just 4-weeks post implantation. We attribute the demonstrated success of this illustrated dual GF-loaded CHA scaffold to its two constituents; namely the biocompatible, bioresorbable and osteoconductive collagen-hydroxyapatite scaffold and the osteoinductive, synergistic effect that rhBMP-2 and rhVEGF

possess in the recapitulation of vascular bone tissue. This therapeutic effect is concentrated locally within the defect via the natural affinity of GFs for the ceramic hydroxyapatite component of the composite scaffold (Lo et al., 2012), thereby functioning to create a highly osteogenic scaffold. Our findings suggest that the harnessing of biological cues, in the form of osteogenic-angiogenic coupling can be used to stimulate efficient bone tissue repair using a cell-free, ceramic containing, biomimetic scaffold thereby negating the requirement for supraphysiological dosing levels or complex delivery systems.

Conclusion

In summary, we demonstrate that the inclusion of a ceramic HA component in a CHA scaffold facilitates the sustained release of bioactive, therapeutic proteins over a prolonged period compared to a HA free collagen scaffold *in vitro*. Impressively, this dual GF-loaded CHA scaffold was capable of rapidly regenerating bone tissue *in vivo* using a rodent critical calvarial defect. Full defect bridging was observed in all specimens assessed, with the clear presence of vascularised bone tissue at the very early timepoint of just 4-weeks. The results demonstrate that the CHA scaffold functions to sequester both rhBMP-2 and rhVEGF locally within the defect site, thereby maximising their potential to exert an osteogenic-angiogenic coupling effect and facilitate the use of low overall therapeutic dosing. Overall, we have developed a cell free, biomimetic, dual-GF loaded CHA scaffold which can stimulate rapid bone tissue regeneration *in vivo,* without the requirement for supraphysiological doses of protein or complex delivery systems.

Acknowledgements

This study was undertaken as part of the Translational Research in Nanomedical Devices (TREND) project, School of Pharmacy & Department of Chemistry, RCSI, supported by a Science Foundation Ireland Investigators Program 13/IA/1840 and the Advanced Materials and Bioengineering Research (AMBER) Centre through SFI/12/RC/2278.

Conflict of Interest Statement

The authors have no conflict of interest to declare.

References

Alhag, M., Farrell, E., Toner, M., Lee, T. C., O'Brien, F. J., & Claffey, N. (2012). Evaluation of the ability of collagen-glycosaminoglycan scaffolds with or without mesenchymal stem cells to heal bone defects in Wistar rats. *Oral Maxillofac Surg, 16*(1), 47-55. doi:10.1007/s10006-011-0299-0

Ben-David, D., Srouji, S., Shapira-Schweitzer, K., Kossover, O., Ivanir, E., Kuhn, G., . . . Livne, E. (2013). Low dose BMP-2 treatment for bone repair using a PEGylated fibrinogen hydrogel matrix. *Biomaterials, 34*(12), 2902-2910. doi:http://dx.doi.org/10.1016/j.biomaterials.2013.01.035

Carragee, E. J., Hurwitz, E. L., & Weiner, B. K. (2011). A critical review of recombinant human bone morphogenetic protein-2 trials in spinal surgery: emerging safety concerns and lessons learned. *Spine J, 11*(6), 471-491. doi:10.1016/j.spinee.2011.04.023

Chen, F.-M., Zhang, M., & Wu, Z.-F. (2010). Toward delivery of multiple growth factors in tissue engineering. *Biomaterials, 31*(24), 6279-6308. doi:http://dx.doi.org/10.1016/j.biomaterials.2010.04.053

Curtin, C. M., Tierney, E. G., McSorley, K., Cryan, S. A., Duffy, G. P., & O'Brien, F. J. (2015). Combinatorial gene therapy accelerates bone regeneration: non-viral dual delivery of VEGF and BMP2 in a collagen-nanohydroxyapatite scaffold. *Adv Healthc Mater, 4*(2), 223-227. doi:10.1002/adhm.201400397

David, F., Levingstone, T. J., Schneeweiss, W., de Swarte, M., Jahns, H., Gleeson, J. P., & O'Brien, F. J. (2015). Enhanced bone healing using collagen-hydroxyapatite scaffold implantation in the treatment of a large multiloculated mandibular aneurysmal bone cyst in a thoroughbred filly. *J Tissue Eng Regen Med*. doi:10.1002/term.2006

Dong, X., Wang, Q., Wu, T., & Pan, H. (2007). Understanding Adsorption-Desorption Dynamics of BMP-2 on Hydroxyapatite (001) Surface. *Biophysical Journal, 93*(3), 750-759. doi:https://doi.org/10.1529/biophysj.106.103168

Endo, M., Kuroda, S., Kondo, H., Maruoka, Y., Ohya, K., & Kasugai, S. (2006). Bone regeneration by modified gene-activated matrix: effectiveness in segmental tibial defects in rats. *Tissue Eng, 12*(3), 489-497. doi:10.1089/ten.2006.12.489

Epstein, N. E. (2011). Pros, cons, and costs of INFUSE in spinal surgery. *Surg Neurol Int, 2*, 10. doi:10.4103/2152-7806.76147

Epstein, N. E. (2013). Complications due to the use of BMP/INFUSE in spine surgery: The evidence continues to mount. *Surg Neurol Int, 4*(Suppl 5), S343-352. doi:10.4103/2152-7806.114813

Fröhlich, M., Grayson, W. L., Wan, L. Q., Marolt, D., Drobnic, M., & Vunjak-Novakovic, G. (2008). Tissue Engineered Bone Grafts: Biological Requirements, Tissue Culture and Clinical Relevance. *Current stem cell research & therapy, 3*(4), 254-264.

Geiger, M., Li, R. H., & Friess, W. (2003). Collagen sponges for bone regeneration with rhBMP-2. *Advanced Drug Delivery Reviews, 55*(12), 1613-1629. doi:http://dx.doi.org/10.1016/j.addr.2003.08.010

Gleeson, J. P., Plunkett, N. A., & O'Brien, F. J. (2010). Addition of hydroxyapatite improves stiffness, interconnectivity and osteogenic potential of a highly porous collagen-based scaffold for bone tissue regeneration. *Eur Cell Mater, 20*, 218-230.

Gorbunoff, M. J., & Timasheff, S. N. (1984). The interaction of proteins with hydroxyapatite: III. Mechanism. *Anal Biochem, 136*(2), 440-445. doi:https://doi.org/10.1016/0003-2697(84)90241-0

Haugh, M. G., Murphy, C. M., McKiernan, R. C., Altenbuchner, C., & O'Brien, F. J. (2011). Crosslinking and mechanical properties significantly influence cell attachment, proliferation, and migration within collagen glycosaminoglycan scaffolds. *Tissue Eng Part A, 17*(9-10), 1201-1208. doi:10.1089/ten.TEA.2010.0590

Ingber, D. E., Mow, V. C., Butler, D., Niklason, L., Huard, J., Mao, J., . . . Vunjak-Novakovic, G. (2006). Tissue engineering and developmental biology: going biomimetic. *Tissue engineering, 12*(12), 3265-3283.

Jeon, O., Song, S. J., Kang, S.-W., Putnam, A. J., & Kim, B.-S. (2007). Enhancement of ectopic bone formation by bone morphogenetic protein-2 released from a heparin-conjugated poly(l-lactic-co-glycolic acid) scaffold. *Biomaterials, 28*(17), 2763-2771. doi:http://dx.doi.org/10.1016/j.biomaterials.2007.02.023

Keeney, M., van den Beucken, J. J. J. P., van der Kraan, P. M., Jansen, J. A., & Pandit, A. (2010). The ability of a collagen/calcium phosphate scaffold to act as its own vector for gene delivery and to promote bone formation via transfection with VEGF165. *Biomaterials, 31*(10), 2893-2902. doi:http://dx.doi.org/10.1016/j.biomaterials.2009.12.041

Kim, J. H., Kim, T. H., Jin, G. Z., Park, J. H., Yun, Y. R., Jang, J. H., & Kim, H. W. (2013). Mineralized poly(lactic acid) scaffolds loading vascular endothelial growth factor and the in vivo performance in rat subcutaneous model. *J Biomed Mater Res A, 101*(5), 1447-1455. doi:10.1002/jbm.a.34446

Koh, J. T., Zhao, Z., Wang, Z., Lewis, I. S., Krebsbach, P. H., & Franceschi, R. T. (2008). Combinatorial gene therapy with BMP2/7 enhances cranial bone regeneration. *J Dent Res, 87*(9), 845-849. doi:10.1177/154405910808700906

Lee, K., Silva, E. A., & Mooney, D. J. (2011). Growth factor delivery-based tissue engineering: general approaches and a review of recent developments. *J R Soc Interface, 8*(55), 153-170. doi:10.1098/rsif.2010.0223

Lo, K. W. H., Ulery, B. D., Ashe, K. M., & Laurencin, C. T. (2012). Studies of bone morphogenetic protein-based surgical repair. *Advanced Drug Delivery Reviews, 64*(12), 1277-1291. doi:https://doi.org/10.1016/j.addr.2012.03.014

Lyons, F. G., Al-Munajjed, A. A., Kieran, S. M., Toner, M. E., Murphy, C. M., Duffy, G. P., & O'Brien, F. J. (2010). The healing of bony defects by cell-free collagen-based scaffolds compared to stem cell-seeded tissue engineered constructs. *Biomaterials, 31*(35), 9232-9243. doi:10.1016/j.biomaterials.2010.08.056

Lyons, F. G., Gleeson, J. P., Partap, S., Coghlan, K., & O'Brien, F. J. (2014). Novel microhydroxyapatite particles in a collagen scaffold: a bioactive bone void filler? *Clin Orthop Relat Res, 472*(4), 1318-1328. doi:10.1007/s11999-013-3438-0

Martínez-Sanz, E., Ossipov, D. A., Hilborn, J., Larsson, S., Jonsson, K. B., & Varghese, O. P. (2011). Bone reservoir: Injectable hyaluronic acid hydrogel for minimal invasive bone augmentation. *Journal of Controlled Release, 152*(2), 232-240. doi:http://dx.doi.org/10.1016/j.jconrel.2011.02.003

McKay, W. F., Peckham, S. M., & Badura, J. M. (2007). A comprehensive clinical review of recombinant human bone morphogenetic protein-2 (INFUSE(®) Bone Graft). *International Orthopaedics, 31*(6), 729-734. doi:10.1007/s00264-007-0418-6

O'Brien, F. J., Harley, B. A., Yannas, I. V., & Gibson, L. (2004). Influence of freezing rate on pore structure in freeze-dried collagen-GAG scaffolds. *Biomaterials, 25*(6), 1077-1086.

O'Loughlin, P. F., Morr, S., Bogunovic, L., Kim, A. D., Park, B., & Lane, J. M. (2008). Selection and development of preclinical models in fracture-healing research. *J Bone Joint Surg Am, 90 Suppl 1*, 79-84. doi:10.2106/jbjs.g.01585

Ono, I., Yamashita, T., Jin, H.-Y., Ito, Y., Hamada, H., Akasaka, Y., . . . Jimbow, K. (2004). Combination of porous hydroxyapatite and cationic liposomes as a vector for BMP-2 gene therapy. *Biomaterials, 25*(19), 4709-4718. doi:https://doi.org/10.1016/j.biomaterials.2003.11.038

Park, J., Lutz, R., Felszeghy, E., Wiltfang, J., Nkenke, E., Neukam, F. W., & Schlegel, K. A. (2007). The effect on bone regeneration of a liposomal vector to deliver BMP-2 gene to bone grafts in peri-implant bone defects. *Biomaterials, 28*(17), 2772-2782. doi:10.1016/j.biomaterials.2007.02.009

Patel, Z. S., Young, S., Tabata, Y., Jansen, J. A., Wong, M. E. K., & Mikos, A. G. (2008). Dual delivery of an angiogenic and an osteogenic growth factor for bone regeneration in a critical size defect model. *Bone, 43*(5), 931-940. doi:http://dx.doi.org/10.1016/j.bone.2008.06.019

Patterson, J., Siew, R., Herring, S. W., Lin, A. S. P., Guldberg, R., & Stayton, P. S. (2010). Hyaluronic acid hydrogels with controlled degradation properties for oriented bone regeneration. *Biomaterials, 31*(26), 6772-6781. doi:http://dx.doi.org/10.1016/j.biomaterials.2010.05.047

Peng, H., Wright, V., Usas, A., Gearhart, B., Shen, H. C., Cummins, J., & Huard, J. (2002). Synergistic enhancement of bone formation and healing by stem cell-expressed VEGF and bone morphogenetic protein-4. *J Clin Invest, 110*(6), 751-759. doi:10.1172/jci15153

Quinlan, E., López-Noriega, A., Thompson, E., Kelly, H. M., Cryan, S. A., & O'Brien, F. J. (2015). Development of collagen–hydroxyapatite scaffolds incorporating PLGA and alginate microparticles for the controlled delivery of rhBMP-2 for bone tissue engineering. *Journal of Controlled Release, 198*, 71-79. doi:http://dx.doi.org/10.1016/j.jconrel.2014.11.021

Quinlan, E., Lopez-Noriega, A., Thompson, E. M., Hibbitts, A., Cryan, S. A., & O'Brien, F. J. (2015). Controlled release of vascular endothelial growth factor from spray-dried alginate microparticles in collagen-hydroxyapatite scaffolds for promoting vascularization and bone repair. *J Tissue Eng Regen Med*. doi:10.1002/term.2013

Quinlan, E., Thompson, E. M., Matsiko, A., O'Brien, F. J., & Lopez-Noriega, A. (2015). Long-term controlled delivery of rhBMP-2 from collagen-hydroxyapatite scaffolds for superior bone tissue regeneration. *J Control Release, 207*, 112-119. doi:10.1016/j.jconrel.2015.03.028

Raftery, R. M., Mencia Castano, I., Chen, G., Cavanagh, B., Quinn, B., Curtin, C. M., . . . O'Brien, F. J. (2017). Translating the role of osteogenic-angiogenic coupling in bone formation: Highly efficient chitosan-pDNA activated scaffolds can accelerate bone regeneration in critical-sized bone defects. *Biomaterials, 149*, 116-127. doi:10.1016/j.biomaterials.2017.09.036

Raftery, R. M., Walsh, D. P., Castano, I. M., Heise, A., Duffy, G. P., Cryan, S. A., & O'Brien, F. J. (2016). Delivering Nucleic-Acid Based Nanomedicines on

Biomaterial Scaffolds for Orthopedic Tissue Repair: Challenges, Progress and Future Perspectives. *Adv Mater, 28*(27), 5447-5469. doi:10.1002/adma.201505088

Raftery, R. M., Woods, B., Marques, A. L. P., Moreira-Silva, J., Silva, T. H., Cryan, S.-A., . . . O'Brien, F. J. (2016). Multifunctional biomaterials from the sea: Assessing the effects of chitosan incorporation into collagen scaffolds on mechanical and biological functionality. *Acta Biomaterialia, 43*, 160-169. doi:http://dx.doi.org/10.1016/j.actbio.2016.07.009

Subbiah, R., Hwang, M. P., Van, S. Y., Do, S. H., Park, H., Lee, K., . . . Park, K. (2015). Osteogenic/angiogenic dual growth factor delivery microcapsules for regeneration of vascularized bone tissue. *Adv Healthc Mater, 4*(13), 1982-1992. doi:10.1002/adhm.201500341

Verrier, S., Alini, M., Alsberg, E., Buchman, S. R., Kelly, D., Laschke, M. W., . . . Evans, C. (2016). Tissue engineering and regenerative approaches to improving the healing of large bone defects. *Eur Cell Mater, 32*, 87-110.

Walsh, D. P., Heise, A., O'Brien, F. J., & Cryan, S. A. (2017). An efficient, non-viral dendritic vector for gene delivery in tissue engineering. *Gene Ther*. doi:10.1038/gt.2017.58

Walsh, D. P., Murphy, R. D., Panarella, A., Raftery, R. M., Cavanagh, B., Simpson, J. C., . . . Cryan, S.-A. (2018). Bioinspired Star-Shaped Poly(L-Lysine) Polypeptides; Efficient Polymeric Nanocarriers for the Delivery of DNA to Mesenchymal Stem Cells. *Molecular Pharmaceutics*. doi:10.1021/acs.molpharmaceut.8b00044

Wang, K., Zhou, C., Hong, Y., & Zhang, X. (2012). A review of protein adsorption on bioceramics. *Interface Focus, 2*(3), 259-277. doi:10.1098/rsfs.2012.0012

Wei, G., Jin, Q., Giannobile, W. V., & Ma, P. X. (2007). The enhancement of osteogenesis by nano-fibrous scaffolds incorporating rhBMP-7 nanospheres. *Biomaterials, 28*(12), 2087-2096. doi:10.1016/j.biomaterials.2006.12.028

Yilgor, P., Tuzlakoglu, K., Reis, R. L., Hasirci, N., & Hasirci, V. (2009). Incorporation of a sequential BMP-2/BMP-7 delivery system into chitosan-based scaffolds for bone tissue engineering. *Biomaterials, 30*(21), 3551-3559. doi:https://doi.org/10.1016/j.biomaterials.2009.03.024

Yuan, H., Zou, P., Yang, Z., Zhang, X., De Bruijn, J. D., & De Groot, K. (1998). Bone morphogenetic protein and ceramic-induced osteogenesis. *J Mater Sci Mater Med, 9*(12), 717-721.

Zara, J. N., Siu, R. K., Zhang, X., Shen, J., Ngo, R., Lee, M., . . . Soo, C. (2011). High doses of bone morphogenetic protein 2 induce structurally abnormal bone and inflammation in vivo. *Tissue Eng Part A, 17*(9-10), 1389-1399. doi:10.1089/ten.TEA.2010.0555

Figure Legends

Figure 1: ***The incorporation of hydroxyapatite into a collagen scaffold facilitates the sustained release of therapeutic proteins over a 30-day period.*** Quantitative assessment of (A) BMP-2 and (B) VEGF protein released from collagen and CHA scaffolds over a 30-day *in vitro* culture period following soak loading of a 5 µg total protein dose per scaffold (2.5 µg BMP-2 and 2.5 µg VEGF) (GF-loaded). Sustained release of both BMP-2 and VEGF proteins was evident for the CHA scaffold compared to the collagen scaffold which is due to the high affinity of these therapeutic growth factors towards the ceramic HA component. Results are expressed as the mean ± SD (n=3).

Figure 2: ***Sustained release of therapeutic growth factors from a CHA scaffold promotes increased MSC mediated osteogenesis compared to GF-loaded collagen scaffolds.*** Following seeding of MSCs, the dual-GF loaded CHA scaffold resulted in the highest level of MSC mediated osteogenesis (Calcium (µg)/scaffold) of all scaffolds assessed at 30 days post seeding. Results are expressed as the mean ± SD (n=3) where *$p<0.05$ & ***$p<0.001$.

Figure 3: ***Accelerated bone tissue regeneration within a critical calvarial defect using a dual growth factor-loaded scaffold.*** Qualitative microCT analysis of excised calvaria for each specimen 4 weeks post implantation into adult male Wistar rats detailing the variation in *de novo* bone formation for (A) GF-free CHA scaffolds & (B) GF-loaded CHA scaffolds (2.5 µg BMP-2 and 2.5 µg VEGF per scaffold). Complete defect bridging was evident for each specimen in the GF-loaded scaffold group. A 6mm region of interest was selected for quantitative analysis of (C) new bone volume, (D) trabecular number, (E) trabecular thickness and (F) trabecular spacing. All GF-loaded scaffold specimens resulted in enhanced bone volume fraction as well as an increased number of thicker trabeculae compared to that of the GF-free scaffold specimens. Results are expressed as the mean ± SD where *$p<0.05$, ***$p<0.001$ & ****$p<0.0001$.

Figure 4: ***Dual GF-loaded CHA scaffolds result in the formation of mature, vascularised bone tissue within each defect***. Histological assessment of excised calvaria for each specimen 4 weeks post implantation into adult male Wistar rats. (A) Representative H&E and MT images of the GF-free CHA scaffold group using (i-ii) H&E staining and (iii-iv) MT staining. (B) Representative images of the GF-loaded CHA scaffold group (2.5 µg BMP-2 and 2.5 µg VEGF per scaffold) using (i-ii) H&E staining and (iii-iv) MT staining. Qualitatively, the dual GF-loaded scaffold group facilitated enhanced *de novo* bone formation. (C) Quantification of the area of new bone formation using histomorphometrical analysis corroborated these results. (D) Significantly enhanced positive staining for CD31 (red fluorescence) was observed within the (ii) GF-loaded scaffolds compared to the (i) GF-free scaffolds. (E) Quantitatively, the GF-loaded CHA scaffold resulted in an increased vessel density compared to the GF-free CHA scaffold. Results are expressed as the mean area (μm^2) of new bone detected within the defect or the average number of vessels per image assessed ± SD where **$p<0.01$ & ****$p<0.0001$.

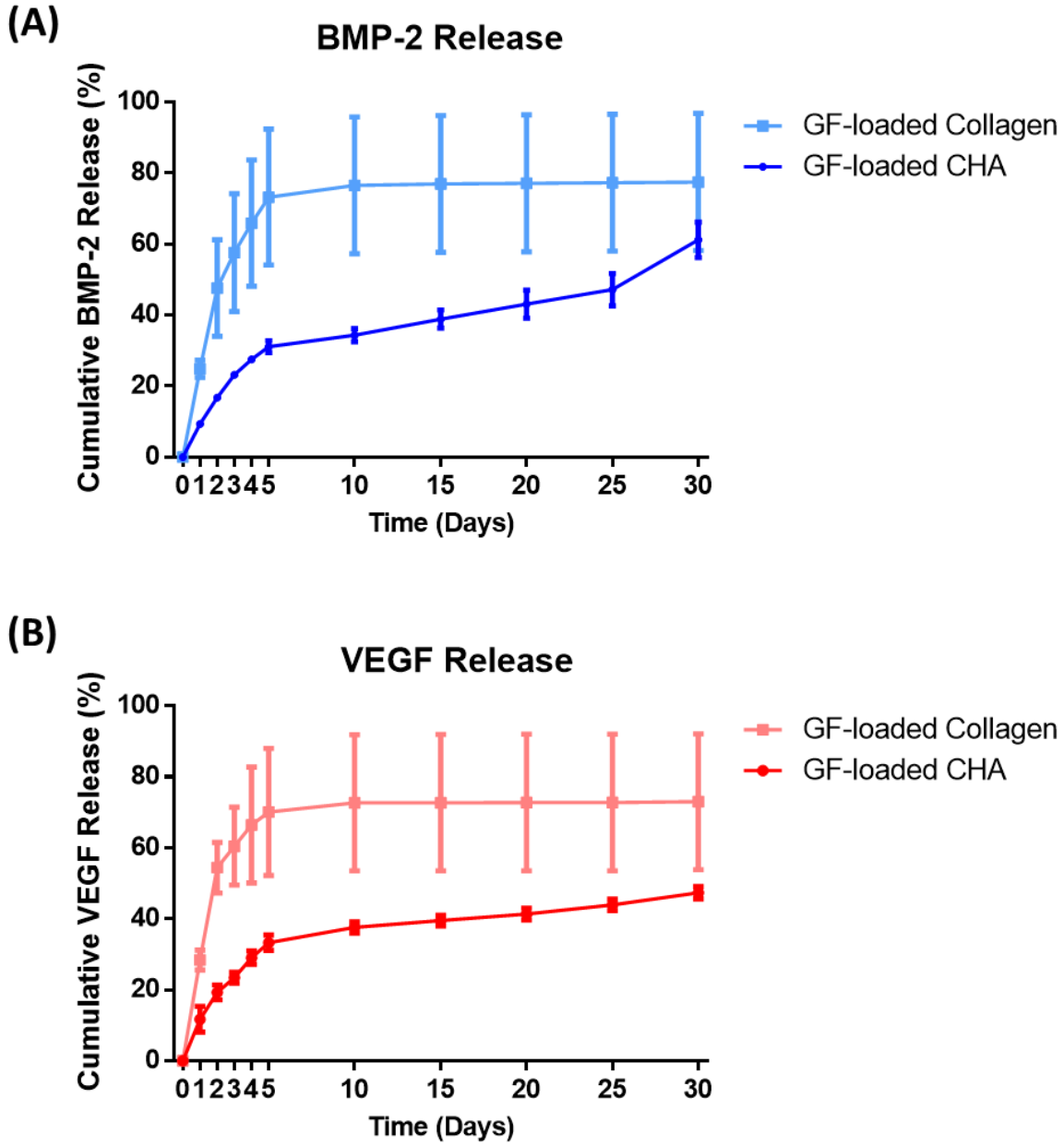

Figure 1: ***The incorporation of hydroxyapatite into a collagen scaffold facilitates the sustained release of therapeutic proteins over a 30-day period.*** Quantitative assessment of (A) BMP-2 and (B) VEGF protein released from collagen and CHA scaffolds over a 30-day *in vitro* culture period following soak loading of a 5 µg total protein dose per scaffold (2.5 µg BMP-2 and 2.5 µg VEGF) (GF-loaded). Sustained release of both BMP-2 and VEGF proteins was evident for the CHA scaffold compared to the collagen scaffold which is due to the high affinity of these therapeutic growth factors towards the ceramic HA component. Results are expressed as the mean ± SD (n=3).

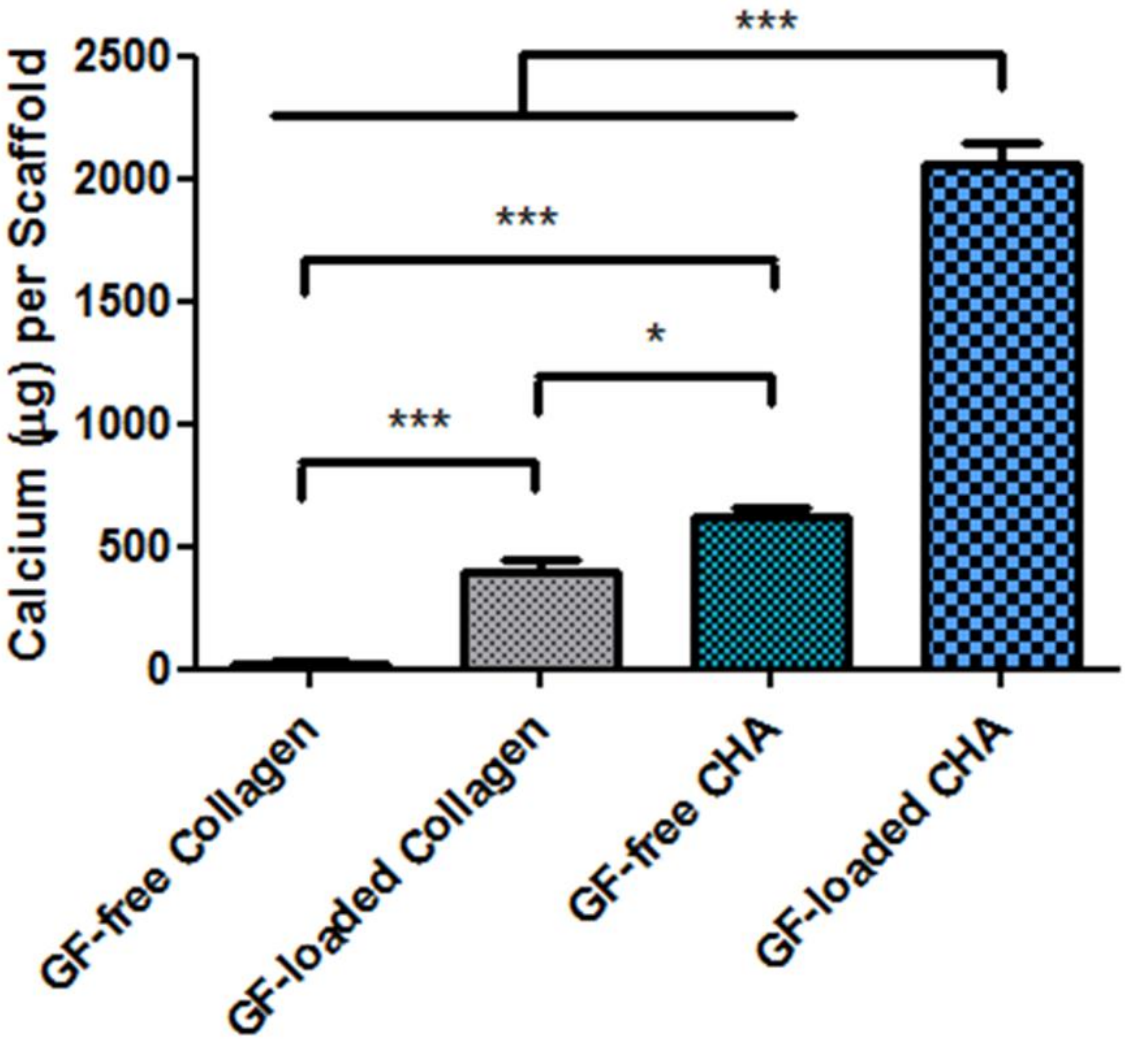

Figure 2: ***Sustained release of therapeutic growth factors from a CHA scaffold promotes increased MSC mediated osteogenesis compared to GF-loaded collagen scaffolds.*** Following seeding of MSCs, the dual-GF loaded CHA scaffold resulted in the highest level of MSC mediated osteogenesis (Calcium (µg)/scaffold) of all scaffolds assessed at 30 days post seeding. Results are expressed as the mean ± SD (n=3) where *p<0.05 & ***p<0.001.

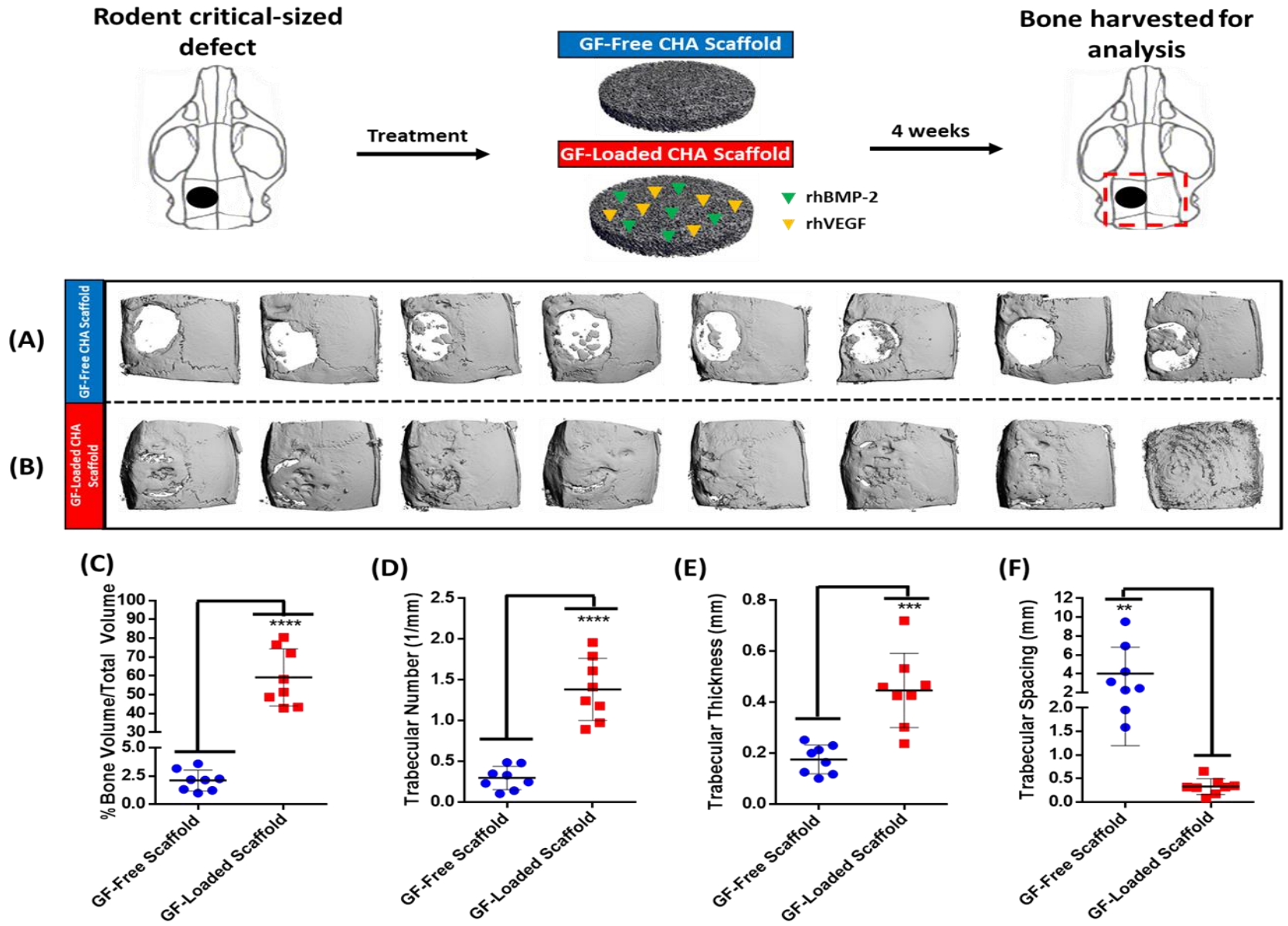

Figure 3: ***Accelerated bone tissue regeneration within a critical calvarial defect using a dual growth factor-loaded scaffold.*** Qualitative microCT analysis of excised calvaria for each specimen 4 weeks post implantation into adult male Wistar rats detailing the variation in *de novo* bone formation for (A) GF-free CHA scaffolds & (B) GF-loaded CHA scaffolds (2.5 µg BMP-2 and 2.5 µg VEGF per scaffold). Complete defect bridging was evident for each specimen in the GF-loaded scaffold group. A 6mm region of interest was selected for quantitative analysis of (C) new bone volume, (D) trabecular number, (E) trabecular thickness and (F) trabecular spacing. All GF-loaded scaffold specimens resulted in enhanced bone volume fraction as well as an increased number of thicker trabeculae compared to that of the GF-free scaffold specimens. Results are expressed as the mean ± SD where *p<0.05, ***p<0.001 & ****p<0.0001.

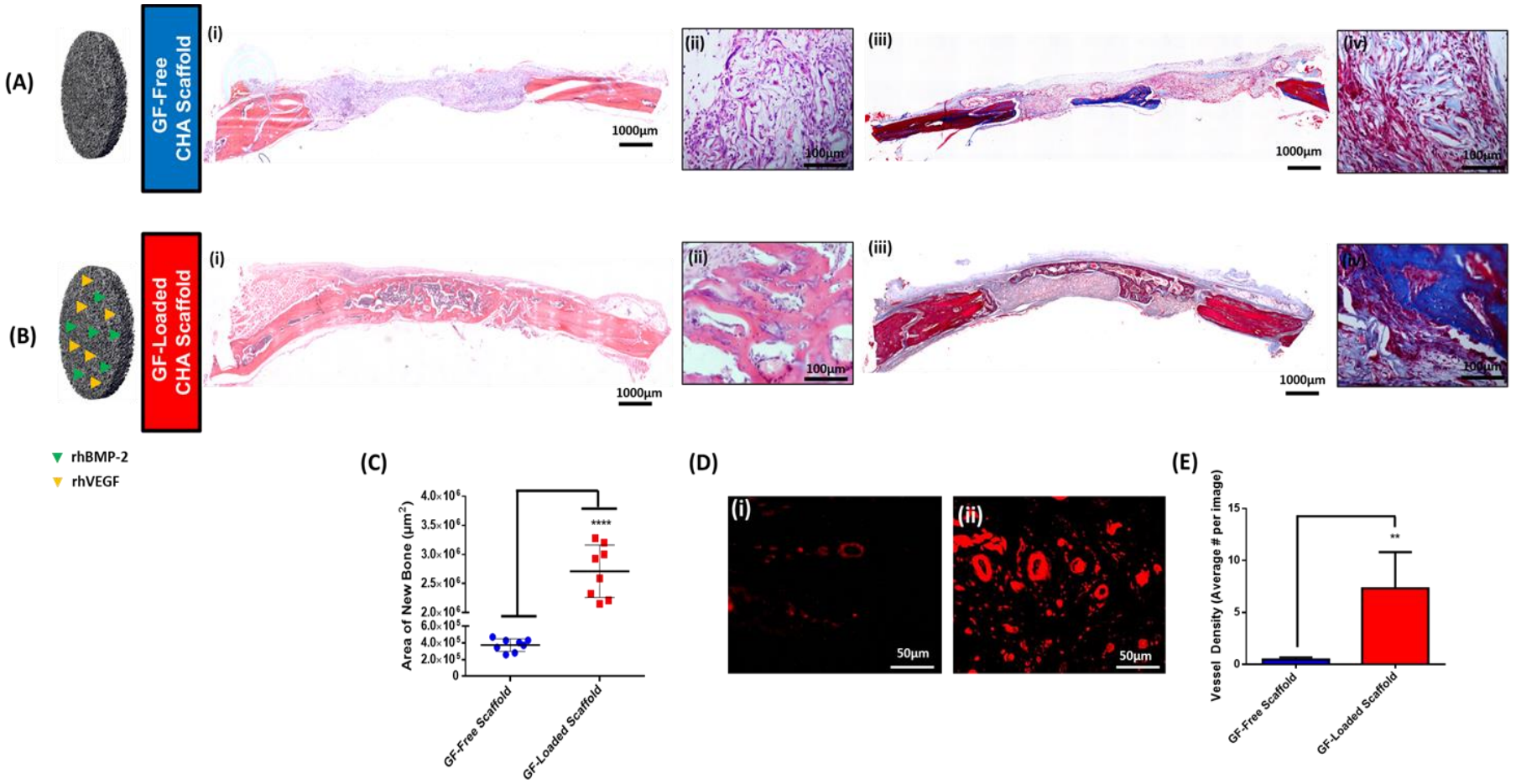

Figure 4: ***Dual GF-loaded CHA scaffolds result in the formation of mature, vascularised bone tissue within each defect***. Histological assessment of excised calvaria for each specimen 4 weeks post implantation into adult male Wistar rats. (A) Representative H&E and MT images of the GF-free CHA scaffold group using (i-ii) H&E staining and (iii-iv) MT staining. (B) Representative images of the GF-loaded CHA scaffold group (2.5 µg BMP-2 and 2.5 µg VEGF per scaffold) using (i-ii) H&E staining and (iii-iv) MT staining. Qualitatively, the dual GF-loaded scaffold group facilitated enhanced *de novo* bone formation. (C) Quantification of the area of new bone formation using histomorphometrical analysis corroborated these results. (D) Significantly enhanced positive staining for CD31 (red fluorescence) was observed within the (ii) GF-loaded scaffolds compared to the (i) GF-free scaffolds. (E) Quantitatively, the GF-loaded CHA scaffold resulted in an increased vessel density compared to the GF-free CHA scaffold. Results are expressed as the mean area (μm^2) of new bone detected within the defect or the average number of vessels per image assessed ± SD where **p<0.01 & ****p<0.0001.